Computers & Fluids 51 (2011) 184–188

Contents lists available at SciVerse ScienceDirect

Computers & Fluids

journal homepage: www.elsevier.com/locate/compfluid

Technical note

Micron particle deposition in the nasal cavity using the v^2–f model

Kiao Inthavong [a], Jiyuan Tu [a,*], Christian Heschl [b]

[a] School of Aerospace, Mechanical and Manufacturing Engineering, RMIT University, PO Box 71, Plenty Road, Bundoora, Victoria 3083, Australia
[b] Fachhochschulstudiengnge Burgenland, University of Applied Science, Steinamangerstraße 21, A-7423 Pinkafeld, Austria

ARTICLE INFO

Article history:
Received 21 September 2010
Received in revised form 15 July 2011
Accepted 22 August 2011
Available online 28 August 2011

Keywords:
Computational fluid dynamics
Eddy interaction model
Particle deposition
Near wall turbulence
Nasal cavity

ABSTRACT

Commercial CFD codes are commonly used to simulate models that involve complicated geometries such as the human nasal cavity. This means that the user has to work within the limitations of the available models of the CFD code. One such issue is the turbulent dispersion of particles in the Lagrangian reference, namely the Discrete Random Walk (DRW) model which overpredicts the deposition of smaller inertial particles, due to its inherent isotropic treatment of the normal to the wall fluctuation, v', in the near wall region. DNS data for channel flows has been used to create a function that reduces the turbulent kinetic energy (TKE) to match the v' profile which has delivered improved particle deposition efficiency results. This paper presents an alternative approach to reduce the TKE to match v', by directly taking the profile from the v^2–f turbulence model. The approach is validated against experimental pipe flow for a 90° bend and then applied to particle dispersion in a human nasal cavity using Ansys-Fluent which showed improved results compared to no modification.

1. Introduction

Particle deposition studies in the human nasal cavity under a laminar flow have been simulated by a number of researchers [1,2]. However for higher breathing rates, the flow field can exist in the turbulent flow regime leading to turbulent dispersion of particles. Reynolds Averaged Navier Stokes (RANS) based turbulence models are often used to resolve the flow field, as it provides simpler and quicker modelling over the more computationally intensive Large Eddy Simulations. However this comes at an expense in that the RANS models, except for the Reynolds Stress Model, fails to resolve the turbulence dissipation and anisotropy which has great significance in the near wall regions of wall bounded flows (i.e. fixed stationary surfaces or boundaries). In particular is the normal to the wall fluctuation, v' which is much smaller than the decomposed value obtained from $u' = v' = w' = \sqrt{2k/3}$. This error propagates to the Lagrangian particle tracking when dealing with the turbulent dispersion, and leads to higher deposition of smaller inertial particles.

To alleviate this problem Liu et al. [3] showed that by damping the turbulent kinetic energy (TKE) in the near wall region, based on the v' profile obtained through DNS data of channel flows [4,5], predictions of the deposition efficiency of micron particles in the human nasal cavity is improved. The new fluctuating velocities are based on the damped TKE to achieve the correct v' value based on the DNS data, however u' and w' are reduced from their original profile, due to the isotropy assumption $u' = v' = w'$. Despite this particle deposition onto wall bounded surfaces, v' is the main contributor to particle deposition by inertial impaction, and therefore a compromise is made to improve the deposition efficiency, when using commercial CFD codes.

In this paper instead of relying on DNS channel flow data that is obtained at Reynolds numbers that do not necessarily match the problem at hand; the v' profile is obtained directly from the flow field using the v^2–f model [6] and is used as the profile for damping the TKE in the Lagrangian particle tracking model. The commercial CFD package, Ansys-Fluent is used to simulate a steady inhalation flow rate of 20 L/min and the one-way coupling of particles under a turbulent flow field. The results arising from the nasal cavity application will contribute towards a better understanding of what causes particles to either deposit early in the nose or bypass the initial airway route completely. Greater knowledge of particle dynamics may also lead to safer guidelines in the context of exposure limits to toxic and polluted air.

2. Method

2.1. Computational model and numerical setup

There are two 90° curvatures in the nasal cavity, one located just after the nostril entrance, and the other at the nasopharynx region (Fig. 1). These two bends act as a naturally occurring filter system that traps high inertial particles as they travel through the airway. A simpler test case for evaluating the CFD models is to

* Corresponding author. Tel.: +61 3 9925 6191; fax: +61 3 9925 6108.
E-mail addresses: kiao.inthavong@rmit.edu.au (K. Inthavong), jiyuan.tu@rmit.edu.au (J. Tu), christian.heschl@fh-pinkafeld.ac.at (C. Heschl).

0045-7930/$ - see front matter Crown Copyright © 2011 Published by Elsevier Ltd. All rights reserved.
doi:10.1016/j.compfluid.2011.08.013

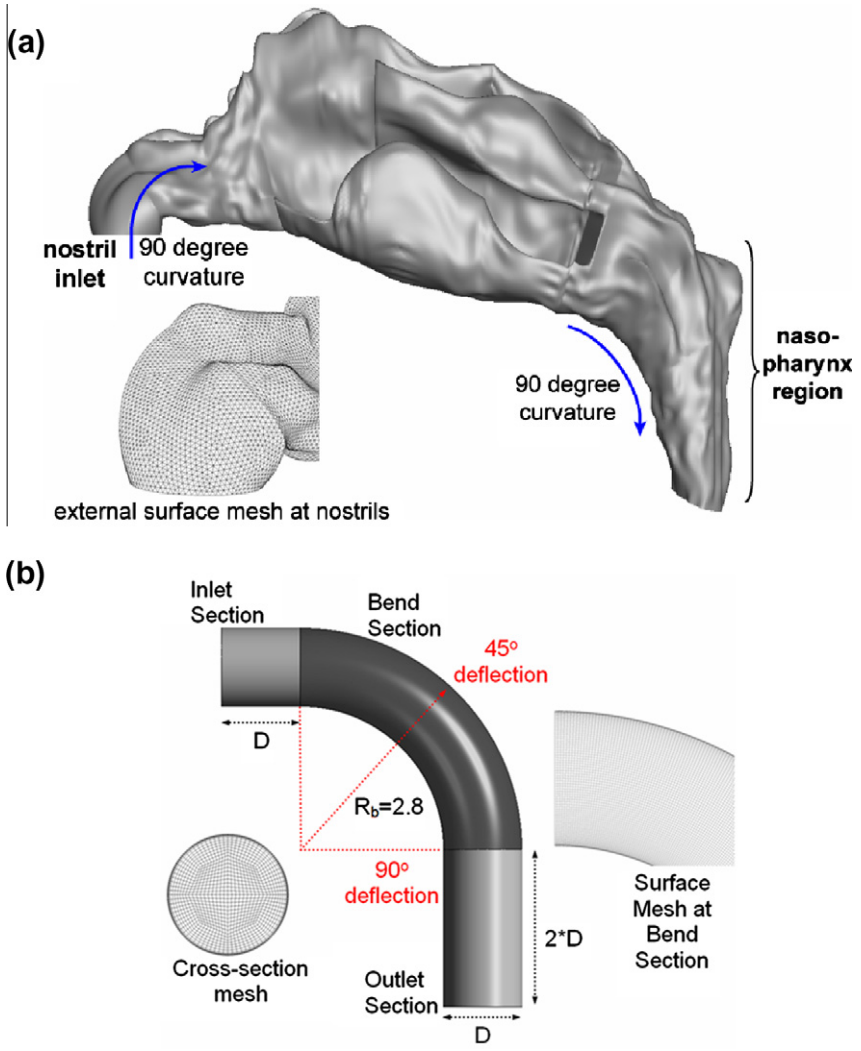

Fig. 1. (a) Lateral view of the nasal cavity model showing the left cavity side. Two 90° curvature bends are present; one at the nostril inlet and the other at the nasopharynx region. The external surface mesh at the nostril inlet is given. (b) Lateral view of the 90° bend pipe. Particle deposition is taken for the Bend section only. D is the pipe diameter (0.02 m); R_b is the radius of curvature of the bend (5.6 cm). A structure mesh with inflation in the near wall region is used.

use a 90° bend pipe based on experimental [7] and Large Eddy Simulation [8] data (Fig. 1). The computational pipe model (0.6 million cells) has a diameter of 0.02 m, radius of curvature R_b = 0.056 m, a curvature ratio of R_o = 5.6, Re = 10,000 and De = 4225. For the human nasal cavity, CT scans of a healthy 25 year old, Asian male, 170 cm height, 75 kg mass provide a three-dimensional outline. An initial model with 260,000 unstructured tetrahedral cells was refined until the skewness of the cells and y^+ value on the walls reached 0.8 and 0.78 respectively. After grid independence and mesh refinements in regions of large flow gradients, near wall cell clustering, smoothing skewed and warped cells, the final model consisted of 3.5 million cells which used a HPxw6600 16 Gb RAM, 8 processor workstation to perform the simulations. The v^2–f model, originally developed by Durbin [6] was implemented in Fluent via user-defined scalar interface. The segregated solver in Fluent is used to solve the additional transport equations for v^2 and f, and the code friendly v^2–f version by Lien and Kalitzin [9] is applied to improve convergence.

For the dispersed phase, each particle is tracked from their initial release point until they escape the domain, terminate or rebound at a surface, or until the integration limit criterion is met. The force balance equation per unit mass of the particle can be given as:

$$\frac{d\vec{u}_p}{dt} = \frac{18\mu_g}{\rho_p d_p^2}\frac{C_d \mathrm{Re}}{24}(\vec{u}_g - \vec{u}_p) + \frac{\vec{g}(\rho_p - \rho_g)}{\rho_p} + \vec{F}_S \quad (1)$$

du_p/dt is the net particle inertia. The terms on the right hand side in order are the drag force, gravity force and additional forces (particle source terms) that are applicable for a given situation involving the dynamics between the particle and the surrounding fluid. The treatment of one-way turbulent dispersion on the particle is performed through the Discrete Random Walk (DRW) or "eddy interaction model" inside Ansys-Fluent. This approach assumes that a particle interacts with a succession of random discrete turbulent eddies, where each eddy is defined by a lifetime, length, and velocity scale [10]. The velocity scale is determined by a Gaussian distributed random velocity fluctuation as:

$$\vec{u}_e = \zeta(2k/3)^{0.5} \quad (2)$$

where ζ is a random Gaussian random number with mean zero and unit variance.

In the turbulent core region, the isotropic assumption is valid in the absence of high swirls and rapid changes in the strain rate; however close to the wall, the turbulent flow character is highly anisotropic.

In an earlier study by the authors [11], a combined mean flow (laminar) tracking and DRW tracking was used for low and high inertial particles respectively. An improved model for the random walk method is proposed by Wang and James [12] and applied in Matida et al. [13] using a damping function applied up to y^+ of 30. With the v^2–f model, the v' profile may be obtained directly from the flow field and is used to modify the TKE as:

$$k_{\text{modified}} = 3v^2/2 \quad \text{for } y^+ < 30 \tag{3}$$

Fig. 2 summarises the two approaches that are used in this paper; *Approach 1* is using the CFD code as is, without modifying the TKE before it is used in the Lagrangian tracking, and *Approach 2* is applying the modification given in Eq. (3) before using it in the Lagrangian tracking. The number of particles tracked was checked for statistical independence since the turbulent dispersion is modelled based on a stochastic process. Independence was achieved for 40,000 particles since an increase of particles to 60,000 particles yielded a difference of 0.1% in the inhalation efficiency. To achieve the uniform particle concentration assumption, particles were released at the same velocity as the freestream. It is assumed that the particles will not affect the fluid flow (one-way coupling) as the volume fraction of the particles was relatively low (<10%). Other assumptions include: (i) no particle rebounding off the walls/surfaces; (ii) no particle coagulation in the particle deposition process and (iii) all particles are spherical and non-deforming.

3. Results and discussion

3.1. Particle deposition in a 90° bend pipe

The predicted deposition of 1–30 μm particles in a 90° bend pipe compared with the experimental data of Pui et al. [7] is shown in Fig. 3. The particle Stokes number is defined as:

$$\text{St} = \frac{\tau_p}{\tau_f} = \frac{\rho_p d_p}{18\mu_g}\frac{U}{D} \tag{4}$$

which is a ratio of the particle relaxation time $\tau_p = \frac{\rho_p d_p}{18\mu_g}$ to the flow characteristic time $\tau_f = \frac{D}{U}$, where U is the mean velocity at the pipe inlet and D is the diameter of the pipe. Secondary flows produced after the bend will force particles in the core pipe region to accelerate towards the outer pipe wall, increasing the inertial impactability. In addition the inertial impaction of particles with small Stokes number (St < 0.1) will be significantly affected by the near wall turbulence whereas for larger Stokes number (St > 1.0) the particles are not affected by the flow field turbulence but instead are only affected by the mean flow. For particles with Stokes number in between 0.1 and 1.0, the particles are influenced by larger scales of turbulence especially in the core flow region. The deposition efficiency for the DRW model using *Approach 1* produces an overprediction in the deposition for St < 0.1 (square symbols in Fig. 3).

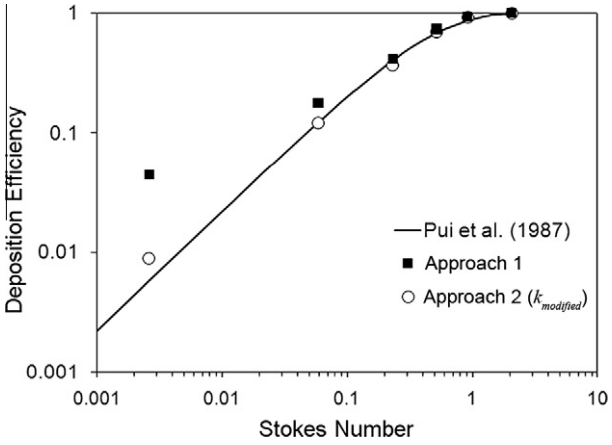

Fig. 3. Particle deposition in a 90° pipe bend for Re = 10,000. The deposition by *Approach 1* and *Approach 2* (k_{modified}) (TKE) are shown. The two approaches are given in Fig. 2.

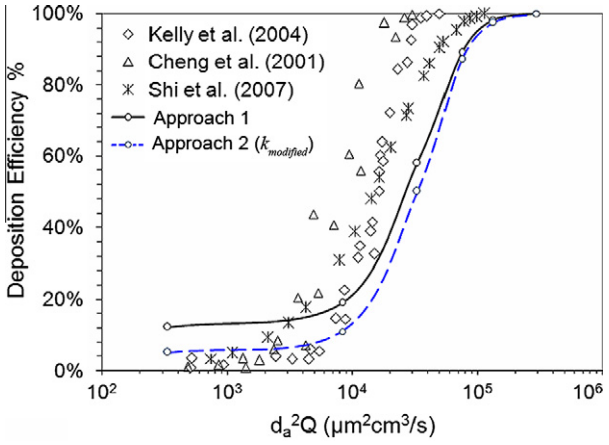

Fig. 4. Comparisons of the inertial particle deposition simulation using the DRW models with the v^2–f turbulence model, against experimental data.

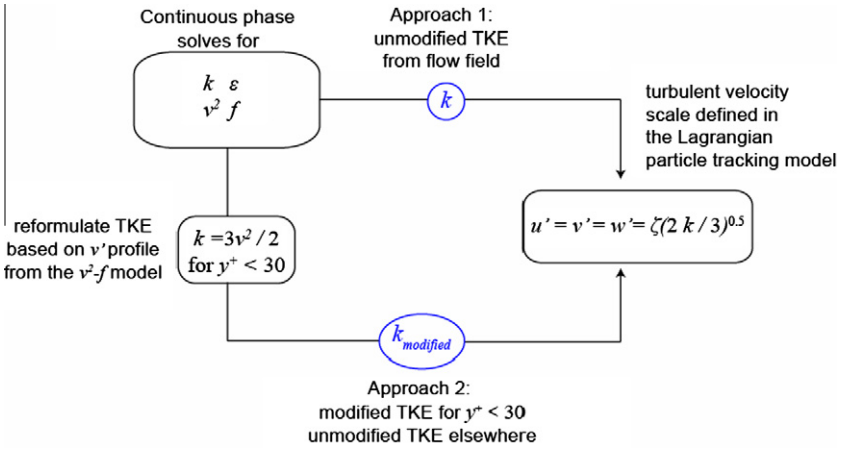

Fig. 2. Schematic of the Lagrangian DRW tracking model. *Approach 1* does not apply any modifications to the TKE. *Approach 2* modifies the TKE from the flow field before passing the modified TKE into the Lagrangian DRW tracking model.

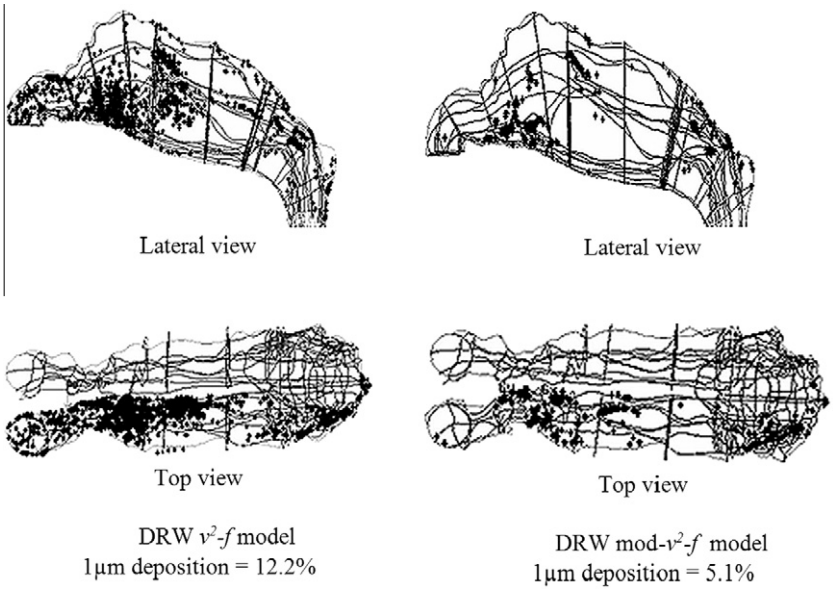

Fig. 5. 1 μm deposition patterns in the nasal cavity for the DRW-v^2–f model and the DRW-Mod-v^2–f model.

The overprediction becomes greater, away from the experimental data as the St decreases further. When the DRW model is modified in *Approach 2*, and the normal fluctuating component takes on the v^2 profile, the deposition efficiency for St < 0.1 is improved.

3.2. Particle deposition in a human nasal cavity

The flow field within the nasal cavity has been resolved and compared with experimental data by the authors in previous studies [14,15] and is not repeated here for brevity, to maintain the focus of the study on particle deposition. The inertial impactability parameter (IP) or particle deposition efficiency curve for a nasal cavity is commonly used to predict the likelihood of particle deposition and is the product of the particle aerodynamic diameter, (d_a = 1, 5, 10, 15, 20, 30 μm) squared, and the inhalation rate (Q = 333.33 cm^3/s).

$$IP = d_a^2 Q \tag{5}$$

The simulated deposition results for a human nasal cavity are compared against experimental data in Fig. 4. It shows that for larger inertial particles ($IP > 10^4$) the predicted deposition efficiency curve is to the right of experimental data (underpredicted). Some possible reasons (which are difficult to control during modelling) include the differences between individual nasal cavity geometries. Also, the surface roughness of experimental models has been shown to influence the deposition data [16] whereas the current CFD simulations assumed smooth walls. Furthermore the fluid velocity within a cell is evaluated through velocity gradients within a computational cell, whereas the DRW model in Ansys-Fluent takes on the cell-centred velocity regardless of its location within the cell. For wall adjacent cells where the velocity gradients are sharp, this can have an influence on the deposition. A near-wall interpolation is then needed to account for this [17]. For smaller inertial particles ($IP < 10^4$) the particle deposition is over predicted and as shown earlier, this can be attributed to the near wall turbulent fluctuations. By reformulating the TKE in *Approach 2*, the normal fluctuating velocity v' is reduced closer to its correct value. This leads to a reduction in the particle deposition for smaller particles, thus improving the DRW tracking in the smaller inertial region. It is also noted that the modification does not have a significant effect on larger inertial particles.

The deposition sites or exact locations of particles can be determined by recording the spatial coordinates when the particle encounters a wall surface. The coordinates of 1 μm particles that deposit or impact onto the nasal cavity walls are recorded and then superimposed onto the nasal cavity geometry as shown in Fig. 5. A large number of particles deposit in the anterior half of the nasal cavity for the 1 μm particle when the DRW model is used. After applying the modification less particles deposit overall (5.1% compared with 12.2%) as well as a large reduction in the anterior half of the nasal cavity. Instead two localised deposition regions are found, one just posterior of the first 90° curvature bend and the second is at the nasopharynx region. The results also suggest that the isotropic assumption in the near wall causes artificial deposition especially in the anterior nasal cavity.

4. Conclusions

The Discrete Random Walk (DRW) model in Ansys-Fluent was used to simulate dispersed particles within a wall-bounded geometry such as the human nasal cavity. A breathing rate of 20 L/min was used and RANS based turbulence models in the form of the v^2–f model was applied. It is well known that when the DRW model is used in conjunction with two-equation RANS turbulence models there is an overprediction of the wall-normal fluctuating velocity component. It was shown that by applying a small modification of $k_{\text{modified}} = 3v^2/2$ directly the DRW can take on a more realistic turbulent dispersion in the near wall region. A 90° pipe bend was used to validate the model which showed an improvement to the particle deposition. The nasal cavity was then used as an application which showed that the modified DRW model provided better matching of the deposition efficiency profile to experimental data for smaller inertial particles through better representation of the turbulence fluctuation. Successful modelling of micron particles will allow more flexibility in simulations of gas-particle flows for inhalation toxicology, and drug delivery studies through the human respiratory system.

Conflict of interest statement

The authors all declare that there is no potential conflict of interest including any financial, personal or other relationships

with other people or organizations within that could inappropriately influence (bias) this work. The paper is an original research article that was financially supported by the Australian Research Council (Project ID LP0989452) and by RMIT University through an Emerging Researcher Grant.

Acknowledgements

The financial support provided by the Australian Research Council (Project ID LP0989452) and by RMIT University through an Emerging Researcher Grant are gratefully acknowledged.

References

[1] Schroeter JD, Kimbell JS, Asgharian B. Analysis of particle deposition in the turbinate and olfactory regions using a human nasal computational fluid dynamics model. J Aerosol Med 2006;19:301–13.
[2] Tian ZF, Inthavong K, Tu JY. Deposition of inhaled wood dust in the nasal cavity. Inhal Toxicol 2007;19:1155–65.
[3] Liu Y, Matida EA, Junjie GU, Johnson MR. Numerical simulation of aerosol deposition in a 3-D human nasal cavity using RANS, RANS/EIM, and LES. J Aerosol Sci 2007;38:683–700.
[4] Moser RD, Kim J, Mansour NN. Direct numerical simulation of turbulent channel flow up to Re[sub tau] = 590. Phys Fluids 1999;11:943–5.
[5] Kim J, Moin P, Moser R. Turbulence statistics in fully developed channel flow at low Reynolds number. J Fluid Mech 1987;177:133–66.
[6] Durbin PA. Near-wall turbulence closure modeling without ‘‘damping functions’’. Theor Comput Fluid Dynam 1991;3:1–13.
[7] Pui DYH, Romay-Novas F, Liu BYH. Experimental study of particle deposition in bends of circular cross section. Aerosol Sci Technol 1987;7:301–15.
[8] Berrouk AS, Laurence D. Stochastic modelling of aerosol deposition for LES of 90° bend turbulent flow. Int J Heat Fluid Flow 2008;29:1010–28.
[9] Lien F, Kalitzin G. Computations of transonic flow with the v2-f turbulence model. Int J Heat Fluid Flow 2001;22:53–6.
[10] Gosman AD, Ioannides E. Aspects of computer simulation of liquid-fuelled combustors. In: AIAA 19th Aerospace sciences meeting. St Louis, MO. 1981. p. Paper AIAA-81-0323.
[11] Inthavong K, Tian ZF, Li HF, Tu JY, Yang W, Xue CL, et al. A numerical study of spray particle deposition in a human nasal cavity. Aerosol Sci Technol 2006;40:1034–45.
[12] Wang Y, James PW. On the effect of anisotropy on the turbulent dispersion and deposition of small particles. Int J Multiphas Flow 1999;25:551–8.
[13] Matida EA, Finlay WH, Lange CF, Grgic B. Improved numerical simulation for aerosol deposition in an idealized mouth-throat. J Aerosol Sci 2004;35:1–19.
[14] Inthavong K, Wen J, Tian ZF, Tu JY. Numerical study of fibre deposition in a human nasal cavity. J Aerosol Sci 2008;39:253–65.
[15] Wen J, Inthavong K, Tu JY, Wang S. Numerical simulations for detailed airflow dynamics in a human nasal cavity. Res Physiol Neurobiol 2008;161:125–35.
[16] Shi HW, Kleinstreuer C, Zhang Z. Modeling of inertial particle transport and deposition in human nasal cavities with wall roughness. J Aerosol Sci 2007;38:398–419.
[17] Inthavong K, Zhang K, Tu J. Numerical modelling of nanoparticle deposition in the nasal cavity and the tracheobronchial airway. Comput method Biomech Biomed Eng 2011.